Article

A theoretical quantum study on the distribution of electrophilic and nucleophilic active sites on Ag(100) surfaces modeled as Finite Clusters

Clara Hilda Rios-Reyes,[1] Rosa Luz Camacho-Mendoza[2] and Luis Humberto Mendoza-Huízar*[2]

[1] Universidad Autónoma Metropolitana-Azcapotzalco, Departamento de Materiales, Av. San Pablo 180, Col. Reynosa Tamaulipas, C.P. 02200 México D.F., México

[2] Universidad Autónoma del Estado de Hidalgo. Centro de Investigaciones Químicas. Carretera Pachuca-Tulancingo km. 4.5, Pachuca, Hgo. CP 42181, México. Tel (+52) 771 7172000 ext 6785, Fax (+52) 771 7172000 ext 6785, e-mail: hhuizar@uaeh.edu.mx

Abstract. A theoretical quantum study on the distribution of electrophilic and nucleophilic active sites on silver surfaces with (100) orientation and modeled as finite clusters is reported. From Hartree-Fock and Density Functional Theory calculations with the LANL1MB and LANL2DZ basis set, we found that the electrophilic active sites are extended and they are formed by a group of atoms. The nucleophilic active sites were located on hollow positions. The numbers of electrophilic and nucleophilic active sites were 1.86×10^{14} and 5.98×10^{14} active sites cm^{-2} respectively.
Keywords: active sites, silver, pseudopotentials, electronic unit cell.

Resumen. Se reporta un estudio teórico cuántico de la distribución de sitios activos electrofílicos y nucleofílicos sobre superficies de plata con orientación (100) modeladas con cúmulos de tamaño finito. A partir de cálculos Hartree-Fock y de la Teoría de los Funcionales de la Densidad con las bases LANL1MB y LANL2DZ encontramos que los sitios electrofílicos son extendidos y formados por un grupo de átomos. Los sitios nucleofílicos se localizaron en posiciones en el hueco. El número de sitios electrofílicos y nucleofílicos fueron 1.86×10^{14} y 5.98×10^{14} sitios-activos cm^{-2} respectivamente.
Palabras clave: sitios activos, plata, pseudopotenciales, celda electrónica unitaria.

Introduction

From its discovery, silver has been used in the production of coins and crafts pieces. At present, silver has been employed in the field of electronics, because it exhibits a high conductivity and their conduction electrons show relatively little resistance to movement under an electric field. Also, their photochemical properties are extensively used in the field of photography [1].

Silver is stable in pure dry air at room temperature, however, it shows high sensitivity to sulfur and its compounds, which are responsible for the familiar tarnishing of the metal (black AgS) when it is exposed to air containing such substances [2]. It has been possible to deposit thin films of Al with different structures onto Ag(100) surfaces, with possible applications in the fabrication of electronic devices [3]. However, during silver deposition on Ag(100), it has been reported the formation of groups of silver atoms as extended islands [3, 4]. There exists evidence of the diffusion processes of these islands or atoms deposited on the silver surface [5, 6]. Although several interpretations have surged in order to explain the phenomena observed on the Ag(100) surfaces, up to our knowledge, there does not exist an explanation based on the exhibited reactivity of the surface. A detailed knowledge of the electronic properties that exhibit the Ag(100) surfaces at atomic level, will allow an important advance in the understanding of the properties and phenomena related to these.

Considerable experimental [7-11] and theoretical [12-14] efforts have been performed in recent years with the intention to explain the electronic properties of silver surfaces.

However, it is unknown yet the factors, at electronic level, responsible for the differences in the reactivity shown by this surface. A good parameter is to find out the number and distribution of active sites on each surface. A typical experimental way to obtain the distribution of these, is to calculate the amount of the adsorbed species and the number of adsorption sites that are associated with the number and distribution of these active sites [15-18]. Others experimental methods involve techniques such as LEED [15], diffraction methods [15, 18], STM 19], etc. However, in most cases a detailed or pin point distribution of the active sites can not be determined. Other methods to determine the number and distribution of active sites on each surface are the theoretical methods [20] which, in most cases, are less expensive than the experimental techniques. Different models have been reported in literature to determine such active sites, employing electrostatic potential [21], embedded cluster [22] and finite clusters [20, 23]. The acceptance of these models is done if these may reproduce the experimental values. Once these have reproduced some experimental properties, the models can be employed to calculate other electronic properties that may not be experimentally obtained. However, the study of the electronic properties of some surfaces is still difficult.

Recently, our group reported a methodology [20, 23] to determine the distribution of active sites on Au(100) surface, employing a cluster of finite size. Using this methodology it was possible to predict the distribution of the actives sites, the work function values, the distribution of the Density of States (DOS) and the band gap, which were very close to the experimental values. In this paper we employ the methodology

reported by us to determine the pin point distribution of active sites onto the Ag(100) surface and analyze the results obtained to gain fundamental knowledge about the reactivity exhibited by the "clean" Ag(100) surfaces. In future studies we will analyze the modification of the reactivity exhibited by silver due an overpotential applied, structural defects, anions and cations adsorbed and the formation of the monolayers of metals onto this surface.

Methodology

Theory

From conceptual Density Functional Theory (DFT), Parr and Yang showed that sites in chemical species with the largest values of Fukui's Function ($f(r)$) are those with higher reactivity. The Fukui´s function is defined as [24]:

$$f(r) = \left(\frac{\partial \rho(r)}{\partial N} \right)_v \tag{1}$$

where ρ is the electronic density, N is the number of electrons and v is the external potential exerted by the nucleus.

There exist two approximations to evaluate the Fukui´s function employing [24]

a) Frontier orbitals (frozen core approximation), and
b) Condensed local softness.

Maps of the HOMO and LUMO

In the first approximation, $f(r)$ can be related with the frontier orbital within the *frozen core* approximation. This approximation considers that when there is a variation on the number of electrons, the respective frontier orbital is only affected, thus when N increases to $N + \mathrm{d}N$:

$$f^-(r) \cong \phi^*_H(r)\phi_H(r) = \rho_H(r), \tag{2}$$

where $\rho_H(r)$ is the electron density of the highest occupied molecular orbital (HOMO).

When N decreases to $N - \mathrm{d}N$,

$$f^+(r) \cong \phi^*_L(r)\phi_L(r) = \rho_L(r), \tag{3}$$

where $\rho_L(r)$ is the electron density of the lowest unoccupied molecular orbital (LUMO).

$f^-(r)$ gives us the more feasible sites (at the reference molecule) to an electrophilic attack while $f^+(r)$ corresponds to a nucleophilic attack.

These approximations, in terms of a frontier orbital, are very valuable because they allow us to study problems of

chemical reactivity by considering only properties of the ground state.

Condensed local softness

In the second approximation, it is possible to define the corresponding condensed or atomic Fukui functions on the jth atom site as,

$$f_j^- = q_j(N) - q_j(N - 1), \tag{4}$$
$$f_j^+ = q_j(N + 1) - q_j(N), \tag{5}$$

for an electrophilic $f_j^-(r)$ or nucleophilic $f_j^+(r)$ attack on the reference molecule, respectively. In these equations, q_j is the atomic charge (evaluated from Mulliken population, electrostatic derived charge, etc.) at the jth atomic site in the neutral (N), anionic (N + 1) or cationic (N - 1) chemical species. Furthermore, since local softness, $s(r)$, is equal to,

$$s(r) = Sf(r), \tag{6}$$

where S is the global softness of the system, $S = \left(\frac{1}{I - A} \right)$, I is the first Ionization potential and A is the electronic affinity, one can similarly define the condensed local softness using Eqs. (4 and 5) in (6) to obtain the respective $s_j^-(r)$ and $s_j^+(r)$. These local reactivity indexes have successfully been applied to rationalize reactivity in a number of chemical situations.

Models

The monocrystalline silver surfaces (100) were modeled as finite clusters of 1, 2, 4 and 8 unit cells containing 14, 23, 38 and 68 atoms respectively, with face centered cubic (fcc) structure, Fig. 1. We have used crystallographic parameters for their construction [25]. All calculations were single point (no further geometry-optimizations) and were carried out at *abinitio* Hartree Fock and DFT levels using the relativistic pseudopotentials (LANL1MB and LANL2DZ) of Hay and Wadt [26,27]. The *effective core potentials* for the silver atoms included relativistic corrections which are known to be important for the transition metals, specially for larger atoms [26].

Computational Resources

We employed a Silicon Graphics OCTANE workstation with 2 processors R10000 and 384 MB of memory, a Silicon Graphics Fuel workstation with processor R14000 and 1 GB of memory and a cluster Beowulf with 6 processors of 2.4 GHZ each one, with 1GB of RAM for all the calculations. These calculations were performed with the package Gaussian 98 ver. A.11 [28] and visualized with the GaussView V. 2.08 [29], Spartan [30] and Gaussumm 9.0 packages [31].
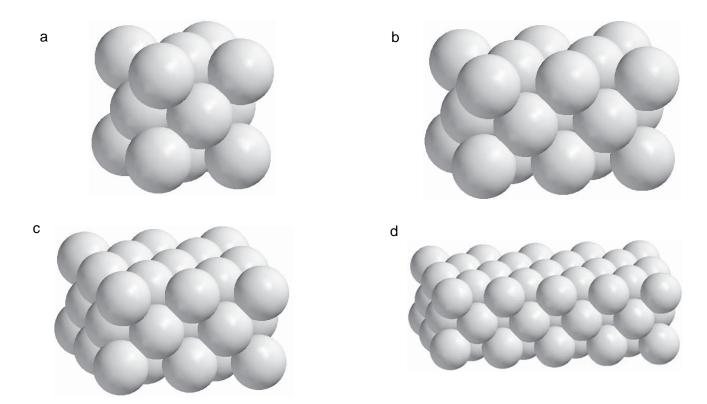
Fig. 1. Clusters models. (a) 1 unit cell (14 atoms), (b) 2 unit cells (23 atoms), (c) 4 unit cells (38 atoms) and (d) 8 unit cells (68 atoms).

Results and discussion

Determination of the cluster size that reproduce some electronic properties of the Ag(100) surface

The reliability of a cluster model generally depends of its ability to reproduce some well known and representative properties experimentally measured. Thus, when the model can reproduce these properties, one can consider that it will predict correctly others properties. In this work we have determined the minimal cluster size of Ag(100) that reproduce correctly the representative properties of a surface: work function, energy gap, and DOS. Once we determined this cluster's size we have employed this model to study the reactivity on the Ag(100) surface.

Work function (w)

Work function is a fundamental electronic property of a metallic surface extremely sensitive to surface conditions. The values of the work function of silver have been measured in air and vacuum conditions. Different experimental work functions values of 'clean' silver surfaces were reported several times in the literature. These values range between 4.1 and 4.8 eV [25, 32-39]. In most of these investigations the state of cleanliness of the surface has not been verified; this has apparently caused the fluctuation in the reported values [32].

The variety in the experimental work function values for silver has motivated several theoretical studies. However, several results reported in literature are ranged between 4.2 and 5.56 eV [40-43]. The values reported depend of the model and the level of theory employed in the calculation. Under the LDA approximation the Ag(100) work function, using no relativistic calculations, yield 4.43 eV [40], 4.38 eV [41] and 5.56 eV [42], while semirelativistic calculations yield 4.77 eV [43]. GGA calculations report 4.2 eV [39] and 5.22 eV [42. From the results mentioned it is easy to observe that the value of the Ag(100) work function, from theoretical studies, is not clear. Up to our knowledge, the relativistic effects have not been considered in the calculation of the Ag(100) work function. At the present work we analyze the influence of the relativistic effects and the cluster size in the work function value.

HOMO´s energy of a finite cluster model can directly be related with the work function of the extended system [20, 44]. Fig. 2 shows the behavior of the HOMO´s energy for the Ag(100) clusters depicted in Fig. 1. The HOMO's energy was calculated employing the basis set LANL1MB (for each Ag atom, the inner shell of 36 electrons respectively is represented by the *effective core potentials* (ECPs) while the valence $4d^{10}5s^1$ electrons are described with a minimum basis set). From Fig. 2, observe that the Ag(100) work function value converges to 4 eV, approximately. Furthermore, one can observe that the work function value can be obtained from the cluster of four unit cells and it is not substantially modified
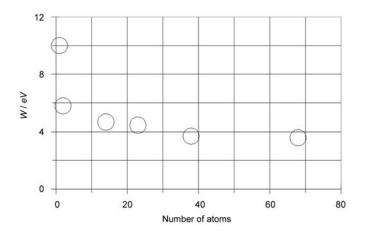
Fig. 2. Work function values for different cluster sizes.

Fig. 3. HOMO–LUMO gaps for different cluster sizes.

when a larger cluster is employed. In a previous work [20], by analogy to the unit cell concept, our group has defined the *electronic unit cell* (EUC) as a finite cluster formed by the minimal number of atoms maintaining a structural (crystallographic) pattern that is capable to model a particular electronic property of certain solids or surfaces. At the present study, the EUC for the Ag(100) surface that reproduces the work function is found to be the cluster of four unit cells.

In order to analyze the effect of the set size basis in the calculations of the work function value, we employed the cluster of four unit cells and the LANL2DZ basis set (for each Ag atom, the inner shell of 28 electrons is represented by the ECPs while the valence $4s^2 4p^6 4d^{10} 5s^1$ electrons are described with a double basis set). The value obtained was 3.9 eV. Observe that the work function value found from HF/LANL1MB calculations was 4.0 eV. The latter result suggests that it is not critical to include larger basis than LANL1MB in the Ag(100) work function calculations. The obtained value with LANL1MB basis set is close to 4.18 eV, which corresponds to the more recent Ag(100) surface work function experimental value [32]. Note that a 5% error against the experimental value is obtained when the LANL1MB basis set is employed. Moreover, the calculation of the work function value for the four unit cells cluster employing the B3LYP functional [45-47] and the LANL2DZ basis set gives a value of 4.03 eV. Thus, apparently the electronic correlation inclusion is not critical in the calculation of this property when the four unit cells cluster is employed as model.

Energy Gap

Another interesting property for clusters is the energy gap (E_g) between the HOMO and LUMO. In Fig. 3 we plotted E_g for different cluster sizes. Observe that E_g is rather large for $n <$ 38, however for $n > 38$, E_g quickly converges to the value of 2.0 eV. E_g calculated employing HF/LANL2DZ and B3LYP/LANL2DZ with the cluster EUC of four unit cells were 2.0 eV and 2.1 eV, respectively. Thus, in the calculation
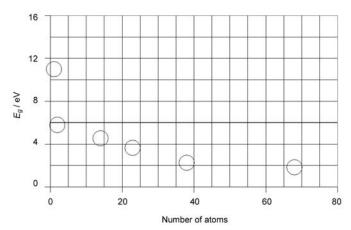
of the E_g for Ag(100) surfaces it is not critical to consider larger basis than LANL1MB and to include the electronic correlation in calculations. Furthermore, the EUC that reproduced the value of the energy gap was the cluster with four unit cells.

Density of states

Density of states (DOS) provides an overall convenient view of the electronic-structure cluster. We further investigated the size dependence of the electronic properties of the silver clusters by the examination of the computed electronic DOS of several representative clusters: Ag_2, Ag_{14}, Ag_{23}, Ag_{38} and Ag_{68} (Fig. 4). Although for the smallest clusters, Ag_2 and Ag_{14}, the energy levels are discrete and peaks are clearly separated, the d and sp energy levels are gradually broadened for Ag_{14}. As the cluster size further increases, for $n > 23$; the d and sp levels broaden out, shift, and overlap with other. Thus, continuous electronic bands are found from $n > 23$; suggesting a solid behavior. Observe that the band gap between valence band and conduction band converge to the 2.0 eV value. Therefore, our modeled surface begins to reproduce the experimental behavior when we employed 23 atoms in our calculations and this behavior is clearly reproduced when we have a four unit cells cluster (38 atoms). No appreciable changes were observed when the cluster size was increased to eight unit cells, neither when the level of calculations HF/LANL2DZ and B3LYP/LANL2DZ were employed.

Observe that the work function value, energy gap and DOS converged when the cluster size was of four unit cells. Therefore, this cluster size may be employed to calculate the electronic properties with enough reliability. Note that we have used a HF/LANL1MB level; however, the results obtained compare favorably with experimental results and with higher levels of theory such as HF/LANL2DZ and B3LYP/LANL2DZ. Thus, with HF/LANL1MB level and by keeping the fixed lattice parameters, it is possible to predict the reactivity shown by the Ag(100) surface, employing a four unit cells cluster.
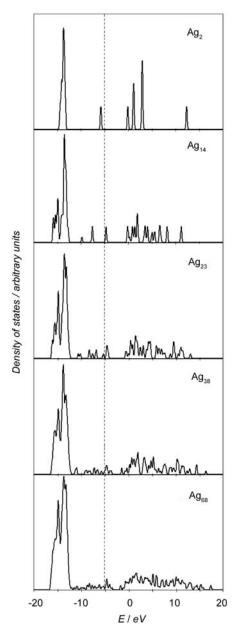
Fig. 4. Density of states (DOS) for different cluster sizes keeping the structure fcc and (100) orientation. Gaussian broadening of 0.05eV is used. Gaussian broadening of 0.05eV is used. Fermi's energy value is shown in Figure as a broken line.

Determination of the active sites on Ag(100) surfaces modeled as Finite Clusters

Electrophilic active sites from silver clusters of 1 ,2, 4 and 8 unit cells at HF/LANL1MB level

From last section it is possible to note that the work function, band gap and DOS Spectrum converge when the EUC four unit cells cluster ($n = 38$) is employed. Note that the results have not appreciably changed when the cluster size was

increased (up to n = 68 atoms). Thus, the four unit cell cluster allow us to obtain the representative distribution of electrophilic sites exhibited by the Ag(100) surfaces. For sake of clarity we have included the analysis for all clusters in Fig. 1.

The electrophilic sites distribution in a system can be derived from the frontier orbital theory within the *frozen core* approximation [48], equation (2). In order to determine this distribution, we analyze the sites where the HOMO frontier orbital attains its larger absolute value on the surface for each one of the studied clusters at HF/LANL1MB level.

The ground state HOMO (absolute value) at the HF/LANL1MB level for each of the clusters of 1, 2, 4 and 8 unit cells of Ag(100) is mapped onto a density isosurface (with a value equal to 0.002 e/a.u.^{3}), Fig. 5. The color code indicates the HOMO's values along this surface. So the darker zones, (electrophilic sites), indicate sites amenable for easier attack by charge acceptors while the lighter regions indicate predominant attack by charge donors. Note also that there are nodal zones where the charge donors might attack. These nodal zones suggest a possible path of movement of the charge donor, which might describe species that undergo diffusion on the surface because there are similar energetic situations [23]. Observe that the HOMO distribution for the one unit cell cluster may be considered very artificial due to the frontier effects in this cluster. For the case of two unit cells it is seen that the HOMO is very different to that obtained for one unit-cell cluster. Note that HOMO maps for the two-unit cells cluster suggest no possible electrophilic active sites on this surface indicating a predominant nucleophilic attack onto this surface. This situation probably is due to the frontier effects at this model cluster size. There are two possible ways to take into account the border effects into the calculations; one way is to saturate the valences on the borders of the cluster considering, in artificial way, the effect of the others atoms in the limits of the system [20]. A second way consists in increasing the cluster size until the electronic properties do not change in the center of the cluster, so when the electronic properties converge in this region, we might consider that the effects of the border have been taken into account. We decided to analyze employing the second way. Moreover the results obtained in last section suggest that one may obtain the convergence in the properties from the EUC four unit cells cluster, see Fig. 5. Note that the HOMO's maps for this cluster are different to those shown by the clusters with 1 and 2 unit cells. In the Ag(100) four unit cells cluster, it is possible to identify the existence of one extended active site in the center of the cluster, on top position. The same behavior can be observed in the eight unit cells cluster. Note that if we compare the HOMO maps of the 4 and 8 unit cells Ag(100) clusters, it is possible to observe a periodical relation between the distribution of the electrophilic active sites in both models. These results suggest that the four unit cells cluster is an acceptable EUC to determine the distribution of the electrophilic actives sites onto the Ag(100) surface. Therefore, it is possible to suggest a distribution of electrophilic active sites for a macroscopic Ag(100) surface, by considering the four unit cells
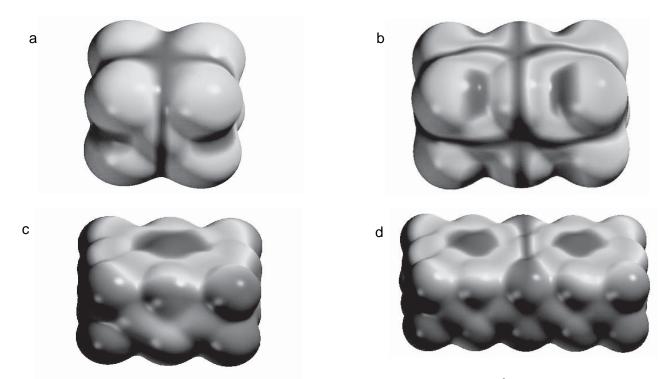
Fig. 5. Mapping of the HOMO at the HF/LANL1MB level onto a density isosurface (value r=0.002 e/a.u.^{3}). Lighter zones have the lower value of HOMO, and darker zones have the higher. (a) 1 unit cell (14 atoms), (b) 2 unit cells (23 atoms), (c) 4 unit cells (38 atoms) and (d) 8 unit cells (68 atoms) clusters.

cluster. Figure 6 depicts a pictorial fraction representation of the macroscopic Ag(100) surface, generated by the four unit cells cluster which is the determined EUC. The number of extended electrophilic active sites counted from Fig. 6 is 1.86 × 10^{14} activesitescm^{-2} and they are located on top positions. This result corresponds to a maximum coverage of 0.25. This prediction is consistent with with a recent experimental report of the formation of a submonolayer of Ag on Ag(100) surface where the coverage was of 25% in a c(4 × 4) structure [49].
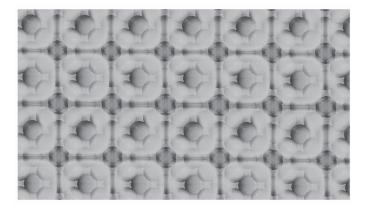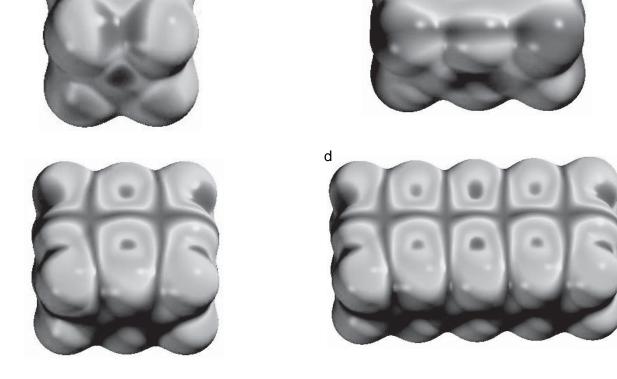

Fig. 6. Pictorial representation of the distribution of electrophilic active sites onto a fraction of the macroscopic (100) silver surface considering the electronic unit cell of a four unit cells cluster.

Nucleophilic active sites from silver clusters of 1, 2, 4 and 8 unit cells at HF/LANL1MB level

The distribution of the nucleophilic active sites in a system can be derived from the theory of frontier orbital within the *frozen core* approximation, too [48], equation (3). We employed the same methodology as in last section to determine the distribution of nucleophilic active sites onto the Ag(100) surface. The ground state LUMO (absolute value) at the HF/LANL1MB level for each of the 1, 2, 4, and 8 unit cells clusters of Ag(100) is mapped onto a density isosurface (with a value equal to 0.002 e/a.u.^{3}), see Fig. 7. The colour code indicates the LUMO's values along this surface. So the darker zones, (nucleophilic sites), indicate sites amenable for easier attack by charge donors while the lighter regions indicate predominant attack by charge acceptors. A periodical relation can be observed between the distributions of the nucleophilic active sites in the clusters of four and eight unit cells. Thus, from last results it is possible to find that the EUC that allows getting the macroscopic distribution of the nucleophilic actives sites is the cluster of four unit cells. Figure 8 shows a pictorial fraction representation of the macroscopic Ag(100) surface, assuming that the four unit cells cluster constitutes the EUC and generated from this EUC. The number of nucleophilic active sites counted from Fig. 8 was 5.98 × 10^{14} activesitescm^{-2} and they are located on hollow positions. This result suggests that if small nucleophilic atoms are adsorbed on the Ag(100) surfaces, the maximum coverage would be 0.5

a

b

c

d

Fig. 7. Mapping of the LUMO at the HF/LANL1MB level onto a density isosurface (value r=0.002 e/a.u.^{3}). Lighter zones have the lower value of LUMO, and darker zones have the higher. (a) 1 unit cell (14 atoms), (b) 2 unit cells (23 atoms), (c) 4 unit cells (38 atoms) and (d) 8 unit cells (68 atoms) clusters.

in a c(2x2) structure. This prediction compares favourably with a recent experimental report of the bromide and chloride adsorption onto Ag(100) surfaces [50, 51].

Electrophilic condensed local softness
in the four unit cells cluster

From Fig. 5, one can observe in the 4 and 8 unit cells cluster that the electrophilic active sites are extended in the center of the cluster. In order to analyze this situation, we determined the pin point distribution of this reactivity. It is possible to find such distribution employing the condensed local softness, equation (4). In this work we employed the charges obtained from electrostatic potentials (MEP) because are better than the Mulliken populations to estimate the condensed reactivity indexes [52]. It is important to mention that when a cluster is employed, an internal redistribution of the charge there exists due to the frontier effects. However, when one increases the cluster size to consider the effects of the border (see discussion in section of electrophilic active sites of this paper), the differences in the obtained values of the charges between the clusters of four and eight unit cells were close to 3 %. This result suggests that the four unit cell reproduces the charge

distribution in the center of the cluster. The electrophilic condensed local softness values obtained for each atom at HF/LANL1MB level are shown in Fig. 9. The more reactive sites have values of 0.71, 0.48, 0.37, 0.32 and 0.28 eV. Note that the reactivity of the cluster is located in the center. However, it is possible to observe that the reactivity is slightly displaced to the left side. The characteristic distribution in the
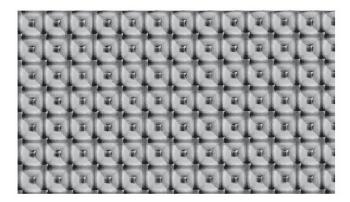
Fig. 8. Pictorial representation of the distribution of nucleophilic active sites onto a fraction of the macroscopic (100) silver surface considering the electronic unit cell of a four unit cells cluster.
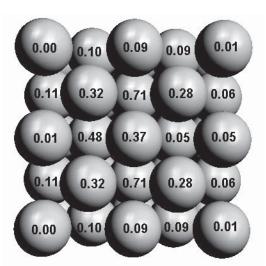
Fig. 9. Condensed local softness values for an electrophilic attack obtained at HF/LANL1MB level. The values are shown in the Figure.

center of the cluster suggests that the proximity of the reactive sites increases the reactivity in this section and the reactivity is given by a group of atoms. This feature indicates that if the Ag(100) surface is attacked by electrophilic agents, the formation of cluster of atoms onto this surface is favored. If one extrapolates this result to the macroscopic surface, it is possible to infer that when the cluster is formed on the reactive group of atoms, the probability of an adsorption out of these is minimal. The above mentioned suggests that the Ag(100) surface favors the formations of "islands of atoms" with a c(4 × 4) distribution. Indeed, last result follows the trend of a recent experimental report of the Ag cluster formation on Ag(100) surface [50].

Conclusions

We determined that the EUC that allows one to properly describe some electronic properties of the Ag(100) surface is the four unit cells finite cluster. From Hartree-Fock and Density Functional Theory calculations with the LANL1MB and LANL2DZ basis, we found that the values of the predicted work function and band gap are 4.0 eV and 2.0 eV, respectively. From the HOMO and LUMO distributions (within the *frozen core* approximation), it was possible to suggest a possible qualitative macroscopic distribution of the electrophilic and nucleophilic active sites, on the modeled Ag(100) surface. We found that the electrophilic active sites are extended and formed by a group of atoms, which favors the formation of islands of atoms onto this surface. The nucleophilic active sites were located on hollow positions. The numbers of electrophilic and nucleophilic active sites were 1.86×10^{14} and 5.98×10^{14} activesitescm^{-2} respectively. These results suggest that the coverage on Ag(100) is 0.25 and 0.5, for the case of electrophilic and nucleophilic attacks with c(4x4) and c(2 × 2) structures, respectively.

References

1. Gould, I. R.; Lenhard, J. R.; Muenter, A. A.; Godleski S. A.; Farid, S. *Pure Appl. Chem.* **2001**, *73*, 455.
2. Cotton, F.A.; Wilkinson, G. *Advanced Inorganic Chemistry*, Wiley/Interscience, New York, fourth ed., **1980**.
3. Fourneé, V.; Ledieu, J.; Cai, T.; Thiel, P. A. *Phys. Rev. B.* **2003**, *67*, 155401.
4. Bardotti, L.; Bartelt, M. C.; Jenks, C. J.; Stoldt, C. R.; Wen, J. M.; Zhang, C.M.; Thiel, P. A.; Evans, J. W. *Langmuir* **1998**, *14*, 1487.
5. Pai, W. W.; Swan, A. K.; Zhang, Z.; Wendelken, J. F. *Phys. Rev. Lett.* **1997**, *79*, 3210.
6. Vidu, R.; Hirai, N.; Hara, S. *Phys. Chem. Chem. Phys.* **2001**, *3*, 3320.
7. Chelvayohan M. and Mee C H B, *J. Phys. C: Solid State Phys.* **1982**, *15*, 2305.
8. Chelvayohan, M. *J. Phys. C: Solid State Phys.* **1983**, *16*, L323.
9. Altieri, S.; Tjeng, L. H.; Voogt, F. C.; Hibma, T.; Rogojanu, O.; Sawatzky, G. A. *Phys. Rev. B.* **2002**, *66*, 155432.
10. Lindroost, M.; Huttunent, P.; Pessat, M.; Hanssonf, G. V.; Karlsson, U. O.; Farrash, A. H. El. *J. Phys. F: Met. Phys.* **1982**, *12*, L71-4.
11. Cuesta, A.; Kolb, D. M. *Surf. Sci.* **2000**, *465*, 310
12. Pacchioni, G. *Electrochim. Acta* **1996**, *41*, 2285
13. Ignaczak, A. *J. Electroanal. Chem.* **2001**, *495*, 160.
14. Gomes, J.A.N.F.; Ignaczak, A. *J. Mol. Struct. (THEOCHEM)* **1999**, *463*, 113.
15. Kleinherbers, K. K.; Janssen, E.; Goldmann, A.; Saalfeld, H. *Surf. Sci.* 1989, *215*, 394.
16. Ocko, B. M.; Wang, J. X.; Wandlowski, Th. *Phys. Rev.Lett.* **1997**, *79*, 1511.
17. Hanewinkel, C.; Otto, A.; Wandlowski, Th. *Surf. Sci.* 1999, *429*, 255.
18. Endo, O.; Kiguchi, M.; Yokohama, T.; Ito, M.; Ohta, T. *J. Electroanal. Chem.* **1999**, *473*, 19.
19. Ocko, B. M.; Magnussen, O. M.; Wang, J. X..; Wandlowski, Th. *Phys. Rev. B* **1996**, *53*, R7654
20. Mendoza-Huizar, L. H.; Palomar-Pardave, M. E; Robles, J. *J. Mol. Struct. (THEOCHEM)* **2004,** 679, 187.
21. Zurita Rubio, J.; Illas F. *Electrochim. Acta* **1995**, *41*, 2275
22. Treesukol, P.; Lewis, J. P.; Limtrakul, J.; Truong, T. *Chem. Phys. Lett.* **2001**, *350*, 128-134.
23. Mendoza Huizar, L. H.; Robles, J.; Silva Domínguez, J. in: Rao, B.K.; Jena, P. (Eds.), *Clusters and Nanostructure Interfaces*, World Scientific, Singapore, 2000, p. 589.
24. Parr, R.G.; Yang, W. *Density-Functional Theory of Atoms and Molecules*, Oxford University Press, New York, 1989.
25. Kittel, C. *Introducción a la Física del Estado Sólido*, Reverte, Barcelona, **1976**.
26. Hay, P.J.; Wadt, W. R. *J. Phys.* **1985**, *82* , 270.
27. Hay, P.J.; Wadt, W. R. *J. Chem. Phys.* **1985**, *82,* 299.

28. Gaussian 98, Revision A.11, Frisch, M. J. ; Trucks, G. W.; Schlegel, H. B.; Scuseria, G. E.; Robb, M. A.; Cheeseman, J. R.; Zakrzewski, V. G.; Montgomery, J. A. Jr.; Stratmann, R. E.; Burant, J. C.; Dapprich, S.; Millam, J. M.; Daniels, A. D.; Kudin, K. N.; Strain, M. C.; Farkas, O.; Tomasi, J.; Barone, V.; Cossi, M.; Cammi, R.; Mennucci, B.; Pomelli, C.; Adamo, C.; Clifford, S.; Ochterski, J.; Petersson, G. A.; Ayala, P. Y.; Cui, Q.; Morokuma, K.; Salvador, P.; Dannenberg, J. J.; Malick, D. K.; Rabuck, A. D.; Raghavachari, K.; Foresman, J. B.; Cioslowski, J.; Ortiz, J. V.; Baboul, A. G.; Stefanov, B. B.; Liu, G.; Liashenko, A.; Piskorz, P.; Komaromi, I.; Gomperts, R.; Martin, R. L.; Fox, D. J.; Keith, T.; Al-Laham, M. A.; Peng, C. Y.; Nanayakkara, A.; Challacombe, M.; Gill, P. M. W.; Johnson, B.; Chen, W.; Wong, M. W.; Andres, J. L.; Gonzalez, C.; Head-Gordon, M.; Replogle, E. S.; Pople, J. A. Gaussian, Inc., Pittsburgh PA, **2001**.

29. Gaussview Rev. 2.08, Version SGI Binary. Gaussian Inc., Pittsburgh, PA.

30. Spartan'02 for Linux package, Wavefunction, Inc., 18401 Von Karman Avenue, Suite 370. Irvine, CA 92612 USA.

31. O'Boyle, N. M.; Vos, J. G. GaussSum 0.9, Dublin City University, 2005. Available at http://gausssum.sourceforge.net

32. Chelvayohan, M.; Mee, C.H.B. *J . Phys. C: Solid State Phys.* **1982**, *15*, 2305

33. Lide, D. R. Ed. *CRC Handbook of Chemistry and Physics* 74th ed.; CRC Press: Boca Raton, Florida, **1993**.

34. Kim, Y. D.; Wei, T.; Wendt, S.; Goodman, D. W. *Langmuir* **2003**, *19*, 7929.

35. Hansson, G. V.; Flodström, S .A. *Phys. Rev. B* **1978**, *17*, 473.

36. Dweydari, A. W.; Mee, C.H. B. *Phys Status Solid.* **1975**, *27*, 223.

37. Michelson, H.B. *J. Appl. Phys* **1977**, *48,* 4729.

38. Abid, J. P.; Girault, H. H.; Brevet, P. F. *Chem. Commun.* **2001**, *9*, 829.

39. Kokalj, A.; Dal Corso, A.; de Gironcoli, S.; Baroni, S. *J. Phys. Chem. B* **2002**, *106*, 9839

40. Methfessel, M.; Hennig, D.; Scheffler, M. *Phys. Rev. B* **1992**, *46*, 4816.

41. Yu, B. D.; Scheffler, M. *Phys. Rev. B* **1997**, *55*, 13916.

42. Yu, B. D.; Scheffler, M. *Phys. Rev. B* **1997**, *56*, R15569.

43. Boisvert, G.; Lewis, L. J.; Puska, M. J.; Nieminen, R. M. *Phys. Rev. B* **1995**, *52*, 9078.

44. Ignaczak, A. *J. Electroanal. Chem.* **2000**, *480*, 209.

45. Becke, A. D. *J. Chem. Phys.* **1993**, *98*, 5648.

46. Becke, A. D. *Phys. Rev. A* **1988**, *38*, 3098.

47. Lee, C.; Yang, W.; Parr, R. G. *Phys. Rev. B* **1988**, *37,* 785.

48. Yang, W.; Parr, R. G.; Pucci, R. *J. Chem. Phys.* **1984**, *81*, 2862.

49. Bardotti, L.; Bartelt, M. C.; Jenks, C. J.; Stoldt, C. R.; Wen, J. M.; Zhang, C. M.; Thiel, P. A.; Evans, J. W. *Langmuir***, 1998,** *14*, 1487.

50. Wandlowski, Th.; Wang, J. X.; Ocko, B. M. *J. Electroanal. Chem.* **2001**, *500*, 418.

51. Wang, S.; Rikvold, P.A. *Phys. Rev. B* **2002**, *65*, 155406.

52. Besler, B. H.; Merz, K.M.; Kollman, P.A. *J. Comp. Chem.* **1990**, *11*, 431.